Distribution Agreement

In presenting this thesis as a partial fulfillment of the requirements for a degree from Emory University, I hereby grant to Emory University and its agents the non-exclusive license to archive, make accessible, and display my thesis in whole or in part in all forms of media, now or hereafter now, including display on the World Wide Web. I understand that I may select some access restrictions as part of the online submission of this thesis. I retain all ownership rights to the copyright of the thesis. I also retain the right to use in future works (such as articles or books) all or part of this thesis.

Alyssa Wu March 30, 2023

Developing a Method for Circulating Tumor Cell Detection in Pediatric Medulloblastoma: Correlations with Metastatic Status and Prognostic Factors

by

Alyssa Wu

Hui Mao
Adviser

Biology

Hui Mao

Adviser

Arri Eisen

Committee Member

Sonal Nalkur

Committee Member

2023

Developing a Method for Circulating Tumor Cell Detection in Pediatric Medulloblastoma: Correlations with Metastatic Status and Prognostic Factors

By

Alyssa Wu

Hui Mao

Adviser

An abstract of
a thesis submitted to the Faculty of Emory College of Arts and Sciences
of Emory University in partial fulfillment
of the requirements of the degree of
Bachelor of Science with Honors

Biology

2023

Abstract

Developing a Method for Circulating Tumor Cell Detection in Pediatric Medulloblastoma: Correlations with Metastatic Status and Prognostic Factors

By Alyssa Wu

Medulloblastoma (MB) is a rare cancer but a leading cause of pediatric brain tumors and is characterized by highly metastatic tendencies and poor prognosis. Literature has evidenced that metastasis includes the movement of circulating tumor cells (CTCs) and circulating tumor cell clusters (CTCCs) throughout a patient's circulatory and lymphatic systems, offering an important potential diagnostic and prognostic for metastasis. Over 90% of cancer-related deaths are attributed to metastasis, yet highly sensitive and specific assays for CTC and CTCC detection have yet to be developed. The purpose of this project was to develop a novel CTC/CTCC detection method for pediatric MB patients and to assess correlations in CTC/CTCC counts and diagnostic and prognostic factors through the combination of antigen-antibody interactions and magnetic nanotechnology. We discovered a statistically positive correlation between CTC concentrations and metastatic status and a predictive threshold for metastasis status composed of the change in CTC concentrations over the course of treatment and disease subtype. Furthermore, we developed a two-predictor predictive probability model of metastasis status. This study demonstrates the promise of CTCs- and nanotechnology-based liquid biopsies as reliable, convenient, non-invasive, and affordable diagnostic and prognostic tools for MB.

Developing a Method for Circulating Tumor Cell Detection in Pediatric Medulloblastoma: Correlations with Metastatic Status and Prognostic Factors

By

Alyssa Wu

Hui Mao

Adviser

A thesis submitted to the Faculty of Emory College of Arts and Sciences

of Emory University in partial fulfillment

of the requirements of the degree of

Bachelor of Science with Honors

Biology

2023

Acknowledgements

I would like to thank every member of the Mao Lab who has supported me throughout the duration of this project and beyond. Thank you to Dr. Yuancheng Li, who helped me with the development of this project and assisted me all throughout. Thank you to Joshua Jones, who trained me in the protocols of this project then proceeded to become my partner as we worked through samples together. Thank you to Dr. Zhengjia Chen, who aided me so immensely in my statistical analyses and answered any and all of my questions. Furthermore, I would like to extend my greatest thanks to my PI, Dr. Hui Mao, who gave me every opportunity to learn and grow in ways I could have never imagined. Thank you also to my incredible and wonderful family who has supported and helped me through everything in every way they could.

Table of Contents

Introduction

Cancer as a Major Public Health Problem

In the past few decades, cancer rates have risen globally and is now the second leading cause of death in the United States, falling only behind heart disease in mortality. Cancer refers to the broad category of diseases characterized by the abnormal, uncontrolled growth and spread of cells. Projections for 2023 estimate that approximately 2 million new cancer diagnoses and 600,000 cancer deaths will occur in the US, and nearly 90% of these deaths are likely to result from the spread, or metastasis, of the patient's primary tumor [1]. This only underscores the necessity of early and accurate detection of metastasis, as delayed diagnosis and subsequent treatments significantly advance disease progress and reduce survival rates.

Circulating Tumor Cells' Role in Metastasis

Metastasis is a complex and multifaceted process with extremely variable pathways and kinetics involved across different cancers [2]. Yet previous literature evidence has identified a key step of metastasis, in which cancerous cells are sloughed off from the primary tumor [3]. These cells are termed circulating tumor cells (CTCs), which may enter a patient's bloodstream and traverse through the circulatory or lymphatic system and lodge in a secondary site to result in metastatic growth; because of the abnormality of tumor vasculature, there are significantly more leaky blood vessels within tumors than typical tissues, which allows for the escape of CTCs [4] (Figure 1). Most CTCs in circulation die, as they must evade immune system responses, mechanical tear and stress, and anoikis, a form of programmed cell death that occurs from detachment from the extracellular matrix (ECM) [5, 6]. Additionally, CTCs may lose their ability to receive signals from the ECM, known as matrix-derived survival signals, that signify microenvironmental conditions to cancer cells, which can influence a cell's gro56wth, differentiation, and ability to evade apoptosis. Yet literature shows that the CTCs that are able to survive circulation may then extravasate from the circulatory or lymphatic system to attach and

colonize at a secondary site, which highlights the importance of CTC in metastasis [7]. Previous studies show that patients with carcinomas, cancers that originate from the epithelium, have survival times that are up to 10 times shorter if ≥3 CTCs were detected, as compared to patients with negative CTC results [8]

CTCs may also be agglutinated and travel in packs, known as circulating tumor cell clusters (CTCCs) or tumor microemboli. While researchers have historically chosen to focus on single CTCs, increasing research on tumor microemboli strongly suggests that the clustering of CTCs leads to increased resistance against immunological attacks and anoikis, as well as more metastatic tendencies [9]. Specifically, the type II interferon, TNF signaling pathways, and antigen processing and presentation pathways of the immune system are down-regulated, while Bc12, the antiapoptotic protein, is up-regulated in clusters as compared to single CTCs [10].

While research has increased in the past few years, there is still uncertainty about the origin of CTC clustering. Collective migration is one popular hypothesis, in which groups of cells travel together via cell-cell junctions; cell-cell junctions are specialized structures that occur in the plasma membrane of cells, which help to physically connect adjacent cells and maintain tissue integrity. They are essential for the organization and communication of cells within tissues and allow for the sensing of guidance signals provided by their microenvironment. Collective migration integrates the leader-follower polarization hypothesis as well, in which there are localized “leader” cells that are followed by “follower” cells that are attached through cell-cell junctions [11] (Figure 2). Leader cells are those that are able to receive and process external guidance signals, which direct these cells in their movement [11]. Literature has indeed shown robust evidence showing that this is one potential mechanism of CTCC genesis and circulation [12]. Furthermore, researchers have hypothesized and validated that CTCCs may also navigate the bloodstream through the assistance of circulating blood molecules, such as macrophages [9]. Studies have shown interactions between CTCs and macrophages that even extend to fusion. These

interactions and fusions can lead to two outcomes: evasion from the immune system or inducement of inflammation, which still assists CTCC migration, as inflammation creates ideal conditions for local extracellular matrix remodeling [9].

Potential of CTC and CTCC Capture for Metastasis Detection

Detecting and enumerating CTCs and CTCCs offers a novel and potentially key method in determining the early presence of metastasis and provides clinical importance for developing more specific treatment plans. Traditional tissue biopsies only sample from a portion of the bulk primary tumor, and given the heterogeneous nature of tumors - and particularly that the heterogeneity increases as a cancer develops [13] - the characterization of collected tissue samples may miss key traits of other areas of the primary tumor, which may hinder a clinician's ability to prescribe effective treatments. This gap in knowledge may be significantly reduced with liquid biopsies and the information that CTCs and CTCCs provide.

The characterization of the detected CTCs and CTCCs could also provide important information for clinicians, given that their phenotype simultaneously reflects the status of the primary tumor and resulting metastatic cells; CTCs often take on small and successive genomic and epigenomic changes that lead to greater malignancy [6]. As such, the capture and evaluation of CTCs and CTCCs can offer an integral dynamic evaluation and monitoring of a patient's cancer progress that is lacking from other current clinical methods [14]. For example, in relation to chemoradiation treatments, a change in the concentration of CTCs after the treatment could help dictate a patient's response and predict the success of systemic treatment methods.

Current CTC and CTCC detection is conducted with blood draws, and the potential for a "liquid biopsy" also presents noteworthy advantages for patients and clinicians alike. Blood draws allow for greater accessibility and ease of collection; CTCs can be obtained from a routine blood draw with minimal risk and inconvenience to the patient in comparison to a standard tissue biopsy. Additionally, a liquid biopsy presents the ability to measure CTCs multiple times, increasing the

personalization of care as well as increasing the chances of early detection. Regarding patients diagnosed with a metastatic tumor, tumor recurrence after treatment can be difficult to detect, and the response and results of systemic treatments would be easier to conclude with the assistance of a liquid biopsy.

Obstacles and Challenges to CTC Capture

While CTC/CTCC capture offers great potential as part of the cancer diagnosis and treatment, the sheer rarity of CTCs - and particularly CTCCs - underscores the technical challenge of catching and identifying these cells, as well as separating them from leukocytes, erythrocytes, and other non-tumor cells with similar tissue origins; for example, 1 mL of blood contains approximately 10 million leukocytes and 5 billion erythrocytes alone. The technical difficulty in capturing the rare population of CTCs partially justified the establishment of $\geq$ 5 CTCs/mL blood serving as the threshold of CTC positivity [15], which is a relatively low level of sensitivity. As such, there is an urgent need to develop better detection methodologies and to identify and validate reliable markers for CTCs.

Current CTC Capture Methods and Their Limitations

Various techniques and technologies have been developed and employed for the enrichment and isolation of CTCs, including size-based, PCR-reliant, density-dependent, and antibody-antigen techniques [15]. Size-based membrane filtration systems can process high-throughput samples with nearly 50-85% recovery but have very poor purity (~0.1%), which often complicates the enumeration process. Recently PCR technology has been shown to be a highly sensitive method capable of detecting one CTC in excess of 10^6 leukocytes [16]. However, this assay tends to have high inter-lab variability and false positive rate and requires highly skilled sample handling and manipulation. Density-based methods typically do not require expensive equipment but require large volumes of blood and are unable to accurately separate white blood

cells from CTCs of similar size [15]. Antibody-antigen interactions are highly specific, as antibodies are designed to recognize and bind to specific antigens according to their molecular shape and cues. Therefore, antibody-antigen interactions offer the most specific and sensitive methods of CTC binding and enrichment [17]. However, the accuracy of this method relies on the identification of robust, reliable, and specific biomarkers for accurate use. Biomarkers for CTCs have been screened and detected, the most notable of which is EpCAM (epithelial cell adhesion molecule), a marker of epithelial cells. Given that 80-90% of cancers originate from epithelial tissue, EpCAM is the most widely used biomarker for detecting CTCs and is utilized in CellSearch®, the only FDA-approved CTC detection and enumeration method, which uses EpCAM antibody-coated ferromagnetic beads to isolate CTCs from a liquid biopsy sample [15] and requires 7.5 mL blood sample to isolate a single CTC. Among CTCs of epithelial tumors, CellSearch® only shows a small fraction of a much larger and significantly heterogeneous cohort of CTCs [18], and typically yields modest to low recoveries of CTCs (~60% by negative depletion and ~25% using positive selection) as well as unfavorable purity (~1%) [19]. In order to obtain a thorough interrogation of each cell in the flow, its CTC Test has also compromised its efficiency, leading to a time-consuming procedure and increasing the inconvenience to the patient; the microfluidic system employed by CellSearch® interrogates every single cell in the flow, which prevents loss of especially rare CTCs; however, the flow rate thus is very slow. Furthermore, given that the CellSearch® methodology captures CTCs using anti-EpCAM antibodies, cancer cells that do not originate from the epithelium evade detection; thus, CellSearch® and other EpCAM-targeting detection methods offer no clinical value for non-epithelial high-impact cancers such as brain tumors. Currently, there are no established markers for CTCs derived from brain tumors [13, 20].

Iron Oxide Nanoparticles and Magnetism

Nanotechnology provides great potential for enhancing the sensitivity of commonly used detection methods, such as fluorescence-based detection, as nanoparticles have characteristically high surface area-to-volume ratios that permit adherence of dense amounts of probing ligands that bind to biomarkers on cancer cells. When nanoparticles are conjugated with a specific antibody against a biomarker, they can be incubated with a blood sample, such that cells, i.e. CTCs, expressing the biomarker can be efficiently separated from the rest of the sample [21, 22]. Therefore, there have been great efforts to pair antibody-based CTC enrichment protocols with various, novel nanomaterials to achieve higher specificity and sensitivity Commonly used nanoparticles for this purpose include quantum dots, aptamers, gold nanoparticles, and magnetic nanoparticles [23-26].

Magnetism is one common method of separation and can be conducted with magnetic nanoparticles, which have magnetic domains poised to align with an external magnetic field [27]. Iron oxide nanoparticles (IONPs) are the most widely used and accepted type of magnetic nanoparticles due to their low toxicity and characteristic superparamagnetic properties, which prevents nanoparticle clustering and aggregation [28]. In practice, once IONPs are conjugated with antibodies that bind to CTCs, an external magnetic field is applied to the blood sample, and nanoparticle-bound cells move in accordance with the field, separating from other non-bound cells in the sample. These cells can then be further isolated for enumeration and characterization (Figure 3).

Medulloblastoma and Recent Findings

Medulloblastomas (MB) are cancerous brain tumors with 350-500 new diagnoses per year in the United States [29-31]. Yet despite its rare occurrence and categorization as a rare cancer type, MB is particularly common in children, is responsible for most pediatric brain tumors (approximately 10%), and is typically diagnosed from ages 5-9 [31].

MB originates in the posterior fossa region of the brain, specifically the cerebellum, and all cases of MB are classified as Grade IV tumors, indicating fast, aggressive, and malignant behavior [31] Mortality from MB is rarely due to the primary tumor but rather by metastases, which occur in approximately 35% of all MB cases and are rarely localized [32].

In the past few years, clinicians and researchers have begun collaborating to classify MB into molecular subtypes, leading to the current four-category subtyping that differentiates based on transcriptional signatures, mutational spectra, copy number profiles, and clinical features [20, 33]. These four groupings are: wingless (WNT), Sonic hedgehog (SHH), Group 3, and Group 4 (Figure 4, Table 1). Clinically, group 3 medulloblastomas are the most aggressive and malignant, and patients diagnosed with this subtype suffer the worst prognosis and survival rates (20-30% 5-year survival rate). Group 3 MB is characterized by the overexpression of *MYC*, a gene that plays a role in cell growth and division, and large-cell anaplastic (LCA) histology. Recently, subclassifications among group 3 MB have been proposed, known as the C1 and C5 subclasses; the C1 subclass is characterized by more frequent *MYC* amplifications and metastasis, yielding a 6-year survival rate of only 21%, as compared to 74% for the C5 subclass.

The SHH and group 4 subtypes exhibit better prognosis than group 3 but are still generally aggressive. Named after the Sonic Hedgehog signaling pathway, which regulates the development of multicellular embryonic cells, SHH medulloblastomas have a higher occurrence in infants (<4 years) and younger children (<15 years). SHH MB embody nearly all desmoplastic medulloblastomas, which are medulloblastomas characterized by the presence of dense, fibrous tissue in the tumor, known as the desmoplasia. 5-year survival rates of SHH range from 65-80%. Group 4 medulloblastomas comprise the largest cohort of MB patients (35%). While this group of MB lacks a distinctive molecular signature compared to the other subtypes, they are generally associated with the overexpression of genes related to neuronal differentiation and offer a 5-year survival rate of 75-90%.

The WNT subtype of MB offers the best prognosis for patients and is characterized by β-catenin nucleopositivity; β-catenin is an evolutionarily conserved molecule that plays regulatory roles in the establishment of the body axis and organ development during embryonic development, as well as tissue homeostasis and cell division in adults. 5-year survival rates for this subtype are 92%, and one study conducted in 2006 by the North American St. Jude Medulloblastoma trials found that 100% (n=10) of patients exhibiting WNT MB had no evidence of disease 5 years after their initial diagnosis, while only 68% (n=59) of patients exhibiting non-WNT MB were in continued remission. Indeed, most deceased patients diagnosed with WNT-type MB succumbed to therapy complications or secondary brain tumors, not from metastatic WNT MB [34].

It was previously believed that brain cancers do not metastasize through peripheral blood but rather cerebrospinal fluid (CSF), as migrating cells from the brain experience the additional challenge of bypassing the highly selective and well-regulated blood-brain barrier [13]. However, further studies with glioblastoma, the most common type of primary brain tumor, surprisingly showed that up to 20% of glioblastoma patients had positive signals for CTCs in peripheral blood samples [13], highlighting the potential for CTC detection in other brain cancers.

Because the majority of MB metastasis is found in the leptomeningeal surface of the brain, it was also previously believed that the spread of MB occurs through the movement of CTCs into and throughout the CSF, but recent studies have also identified CTCs in the blood of therapy-native MB patients [32]; this suggests a potentially promising method of early malignancy detection should specific and sensitive biomarkers for MB CTCs be identified and validated [35].

The Value of Liquid Biopsy for Medulloblastoma

The value of a liquid biopsy for brain tumors is also particularly notable as compared to other solid tumor tissues; the potential complications and risks of traditional tissue biopsy for brain tumors are heightened due to the nature of brain surgeries and may include hemorrhage,

infection, and herniation, all of which are risks of serious nature that are further compounded for patients with comorbidities and other preexisting complications [13]. Repeated tissue biopsies of the brain as a means of monitoring disease progress are also nearly impossible given the invasive, costly, and high-risk nature of the procedure, particularly for MB patients, the majority of whom are children. CTC capture in MB may also be particularly notable, as MB metastases often phenotypically vary significantly from the primary tumor, such that targets and treatments towards the primary tumor have low efficacy rates on secondary growths [32]. Furthermore, liquid biopsies for MB are perhaps even more important than for other brain cancers given the degree to which MB affects children, for whom traditional tissue biopsies and magnetic resonance imaging scans are especially difficult to conduct.

Medulloblastoma Biomarker Identification: Synaptophysin and NCAM

Given the importance of early metastasis detection, it is critical to identify viable biomarkers for MB. One potential biomarker is synaptophysin (SYN), an integral membrane glycoprotein essential for the kinetic regulation of presynaptic vesicles in central nervous system (CNS) neurons. SYN has a tendency for overexpression in medulloblastoma cells [36], and Min et al. have shown that up to 75% of large cell/anaplastic MB, the variant of MB most associated with advanced stage and high mortality disease, overexpress SYN [37], allowing it to serve as a reliable marker for MB in patients. Additionally, given that SYN is a marker for neuronal cells, the capture of any SYN-expressing cells in liquid blood biopsies is highly suggestive of a positive CTC.

Neural cell adhesion molecule (NCAM) is a protein with roles in cell-cell adhesion and neural growth. When present in an altered expression form, NCAM can lead to tumorigenic properties and has also been found to contribute to the development of MB [38]. As such, the presence of synaptophysin and NCAM in the blood serum are likely to be indicative of CTCs, and both may provide important pathways for accurate MB CTC detection. The use of both biomarkers

in detection is both a method of validation of positive signals and serves to capture a greater percentage of CTCs, given the heterogeneous nature of cancer, even when derived from the same tumor sample. Several clinical studies [39, 40] have indeed demonstrated that multiplexed biomarkers, in contrast to a single biomarker, should enhance accuracy in predicting the prognosis of cancer progression and significantly improve clinical decision-making.

Aims of this Project

While there exists literature evidencing the relationship between CTC presence and metastatic cancer, no published data to date have investigated CTC capture in MB patients, nor the possible correlation between CTC concentration and MB prognosis. Given the highly malignant and aggressive nature of MB and the impact of this disease on children, the importance of developing accurate, specific, sensitive, and non-invasive detection methods for MB metastasis cannot be understated. While MB is a rare cancer type, it continues to have detrimental and widespread effects and outcomes on pediatric cancer patients. Yet despite this significant impact on pediatric brain tumor patients, there is little National Institutes of Health (NIH) funding allocated to MB research to investigate MB origins, causes, diagnostic methods, and cures in the private pharmaceutical sector due to its rarity and subsequent low profitability, which only serves to highlight the imperativeness of MB research in the academic sphere. Additionally, while CTC testing from peripheral blood samples promises great clinical value, a lack of standardized guidelines for methodologies limits its current capabilities. Thus, this project aims to identify reliable markers for MB disease, optimize the conditions for CTC capture and isolation, establish standardized protocols for CTC detection for clinical application, and analyze correlations between CTC concentration and MB disease progress among pediatric patients. Based on previous literature, we hypothesize that elevated CTC counts – both baseline and throughout a patient's course of treatment – will correlate with more advanced-stage disease and severe

outcomes and that our proposed methodology will translate to an early metastasis detection method with great clinical promise.

Materials and Methods

Blood and CSF sample preparation

Blood and cerebrospinal fluid (CSF) samples were collected from different stages (M0 - M3) of pediatric medulloblastoma patients under an IRB-approved protocol, Emory University. Each blood and CSF sample was incubated with 100 µL of prepared iron oxide nanoparticles then placed in a magnetic separator to isolate the nanoparticle-infused CTCs from the supernatant. Next, the magnetically separated cells were fixed by incubation in 4% paraformaldehyde for 15 minutes at room temperature, followed by another 1-hour separation in the magnetic separator. After the two separations, each sample was stained with 1 µL (1:200 dilution in 1xPBS) anti-synaptophysin with Alexa Fluor 488 antibody and 4 µL (1:50 dilution in 1xPBS) FITC of anti-NCAM with Alexa Fluor 488 antibody at 4℃ overnight. 0.50 µL Hoechst 33342 Solution was then added to each sample and incubated for 5 minutes at room temperature and in the dark. The sample was then centrifuged at 128 x g for 5 minutes, and the supernatant was removed, and the pellet gently resuspended in one drop of Fluorogel using a 200 µL wide-bore pipette tip and placed in an Ibidi µ-slide VI 0.4 channel slide for fluorescent microscopy.

CTC imaging using Keyence BZ-X810 Widefield Microscope

A navigation map was created using the Navigation Window in the BZ-X software using the x4 lens. An interactive map for quick navigation was generated using automatic scanning. Setting Z position limits was conducted using the x20 lens. The lower limit of Z-Stack was set at ~3150.0 µm, while the upper limit was set at ~3500.0 µm. Exposures were all selected using high-sensitivity resolutions. DAPI exposure was set using the “CH1 Fluor DAPI” channel setting and set between 1/100s and 1/300s, allowing the cells to be viewed without background autofluorescence or oversaturated signaling. FITC exposure was set using the “CH2 Fluor FITC/488” channel setting and set between 1/30s and 1/80s, depending on which exposure time allowed cells to be viewed without background autofluorescence. Brightfield exposure was set

using the “CH4 Bf/Phase” channel setting. Because brightfield is most prone to overexposure, moving to the center of the slide for imaging was critical. Exposure was set at 1/7500s, which is the lowest setting, and illumination was set at 25%, preventing exposure in the center areas of the slide channel. Stitching edge points set the area to be imaged, and multi-color imaging was used for all imaging.

Image Optimizing

To detect positive CTC signals from the fluorescence microscopy, all images were processed through the ImageJ software, which colored FITC-labeled images green, NCAM-conjugated images pink, and DAPI images blue. To determine the brightness threshold for manual enumeration of the microscopy-produced images, FITC-labeled SYN images were overlaid with corresponding DAPI images in Photoshop, and each positive FITC (synaptophysin) signal was cross-checked with a positive DAPI signal to be considered a CTC. The brightness of the negative control sample images was adjusted by -140 in Photoshop, the level at which we detected no positive signals for FITC-labeled SYN, the key biomarker for detecting MB. After adjusting MB patient sample images to this brightness, false-positive synaptophysin signals were still detected, which we determined after cross-checking with the corresponding DAPI channel image. To eliminate these false positive signals, the brightness for the FITC-labeled images were reduced by another -100 in Photoshop (Figures 6 & 7).

CTC and CTCC Enumeration

After image adjustment, a grid was added to each image for ease of manual counting, and positive CTCs signals were circled for future reference and standardization.

Statistical Analysis of Data

All data management and statistical analyses were performed using the SAS statistical package V9.4 (SAS Institute, Inc., Cary, North Carolina). The CTC count, CTC ratio, CTCC count,

CTCC ratio, slope of change in CTC counts, slope of change in CTCC counts were summarized with mean (SD) and median (range). The correlation between the two biomarkers was estimated with Pearson's and Spearman's correlation coefficients and tested with Wald's test. Receiver operator characteristic (ROC) curve analysis was also conducted to analyze the predictive discriminatory powers of change slope of CTC or CTCC alone or in combination with disease subtype on original metastasis. Their abilities to predict original metastasis status were determined by using ROC curves and measuring the area under the curve (AUC). Whether the AUCs of ROC curves were different from 0.5 (which means no discrimination ability) were tested with chi-square tests. The threshold values in the ROC curves were estimated in order to obtain specific sensitivity (such as 90%) and specificity (such as 90%) levels. The significance levels were set at 0.05 for all tests.

Results

Patient Cohort Characterization

Over the course of this project, 22 patients diagnosed with MB were enrolled in this study, along with 10 pediatric cancer-free patients serving as negative controls. The ages of patients ranged from 1.5-22 years, with a mean age of 12.16 years. All four MB subtypes were represented in the study: WNT (3.1%), SHH (25%), and Group 3/4 (40.6%). Among the 22 MB patients, 63.6% (n=14) had no evidence of metastasis upon diagnosis, while 36.4% (n=8) did have evidence of metastasis upon diagnosis; M1 (9.1%), M2 (4.5%), and M3 (22.7%) stages were all represented in the patient cohort (Table 2). Among the 22 MB patients, only one patient progressed in metastatic stages since the start of treatment, with an initial M-status of M0 that progressed to M3 within 2 years after initial diagnosis. All other patients have maintained the same M-status or are in remission over the course of the study. Since the start of the study in 2021, one patient is now deceased.

Descriptive Statistics for CTC and CTCC Counts

Blood samples were collected from the 22 MB patients throughout the course of their treatment, resulting in a total of 69 samples for analysis and CTC detection and enumeration. Two of these samples were processed and analyzed before we decided to investigate CTCCs as well, thus there are a total of 67 samples for CTCC detection and enumeration.

Due to incomplete optimization of the FITC of anti-NCAM protocol and microscopy imaging conditions, e.g., concentration of anti-NCAM antibody to use, imaging exposure time, etc, SYN was the only biomarker used to enumerate CTCs and CTCCs. The following results are thus reported using a single - not multiplex - biomarker.

The mean concentration of CTCs is 90.85 CTC/mL of blood (SD=112.71) with a range of 0-300+ CTC/mL of blood. The mean concentration of CTCCs is 67 CTCC/mL blood (SD=24.63)

with a range of 0-150 CTC/mL (Table 3). Examples of CTC and CTCC collection are shown in Figure 5.

Among the 22 MB patients, we had longitudinal data for 18 patients, which were used to assess the change in CTC/CTCC concentrations over the course of each individual patient's treatment. To do so, a best-fit line was calculated for each patient using the number of days since diagnosis and the corresponding CTC/CTCC concentration for each day. The slope of the best-fit lines is reported as the slope of CTC(C) change; a negative slope of CTC change indicates a general downward trend in the CTC concentration over the course of patient X's treatment, while a positive slope of CTC indicates a general upward trend in the CTC concentration over the course of patient X's treatment. The mean slope of CTC change was -0.706 (SD=3.69), indicating a general decline in CTC counts as the 18 patients underwent therapies and treatments. The mean slope of CTCC change was 4.63 (SD=16.04), indicating a general increase in CTCC counts as the 18 patients underwent therapies and treatments.

Outcomes for the CTC Dataset

Frequency outcomes were individually assessed for the CTC and CTCC datasets. Frequencies of the status of the primary tumor over the course of each patient's treatment were analyzed and grouped into 5 categories: no evidence of disease (NED)/continuous complete remission (CCR), first relapse (R1), second relapse (R2), third relapse (R3), and no change in the primary tumor status. Among all 22 MB patients, 69 blood samples were collected for CTC analysis, yielding primary tumor statuses falling into all 5 categories: NED/CCR (n=14, 20.29%), R1 (n=20, 28.99%), R2 (n=4, 5.80%), R3 (n=3, 4.35%), and no change (n=28, 40.58%) (Table 4).

Frequencies of metastasis status upon each patient's diagnosis of MB were analyzed. All four metastasis statuses were represented in the patient cohort within the CTC dataset: M0/no evidence of metastasis (n=43, 62.32%), M1 (n=5, 7.25%), M2 (n=3, 4.35%), and M3 (n=18, 26.09%) (Table 5).

Frequencies of metastasis statuses over the course of each patient's treatment were also collected, as tumors may increase or decrease in aggressiveness over the course of treatment. All four M-stages were represented in the CTC dataset: M0/no evidence of metastasis (n=36, 52.94%), M1 (n=4, 5.88%), M2 (n=5, 7.35%), and M3 (n=23, 33.82%) (Table 6).

Additionally, the frequencies of each subtype of MB were investigated: SHH (n=26, 37.68%), WNT (n=3, 4.35%), and Groups 3/4 (n=40, 57.97%) (Table 7).

Outcomes for the CTCC dataset

Frequencies for primary tumor status, initial metastasis status at diagnosis, metastasis statuses, and MB subtypes were similarly calculated for the CTCC dataset, yielding the same frequencies.

Association between CTC concentration and primary tumor and metastasis status

In order to determine any potential correlations between the concentration of CTCs and primary tumor status, the Pearson correlation coefficient and Spearman correlation coefficients were calculated. The same statistical analyses were conducted to assess any potential correlation between CTC ratio and primary tumor status.

These analyses were repeated to determine a potential correlation between the concentration of CTCs and metastasis status, as well as CTC ratio and metastasis status.

According to the Pearson correlation coefficient and Wald's test, CTC counts, represented as CTC concentration (CTC/mL of blood) significantly and positively associated with metastasis statuses of M0-M1 ($r = 0.24100$ and $p = 0.0477$). Statistical analyses show no other significant associations between CTC count and CTC ratio with primary tumor status or metastasis status (Table 8).

Association between CTCC concentration and primary tumor and metastasis status

In order to determine any potential correlations between the concentration of CTCCs and primary tumor status, the Pearson correlation coefficient and Spearman correlation coefficients were calculated. The same statistical analyses were conducted to assess any potential correlation between CTCC ratio and primary tumor status.

These analyses were repeated to determine a potential correlation between the concentration of CTCCs and metastasis status, as well as CTCC ratio and metastasis status. According to the Pearson and Spearman correlation coefficient and Wald's test, there are no significant associations between CTCC count and CTCC ratio with primary tumor status or metastasis status (Table 9).

Determining the threshold in terms of the change slope of CTC and CTCC for original metastasis

In order to determine a potential predictive threshold for CTCs as a marker of initial metastasis status, a Receiver Operating Characteristic (ROC) was conducted (Table 10, Figures 8-11). Because the aim is to develop a *predictive* threshold, slopes of change in CTC/CTCC were used instead of raw CTC/CTCC concentrations in order to take the change in CTC/CTCC concentration over time into account. Analysis was conducted under a single-predictor and two-predictor model, the latter of which combined CTC/CTCC change slope and MB disease subtype. Metastasis states were coded into a binary variable, in which 0=M0, and 1=M1/M2/M3.

According to the ROC analyses, the slope of the change in CTC counts or CTCC change slope by itself does not offer significant predictive power of initial metastasis status ($p > 0.05$). Additionally, the combination of CTCC change slope and disease subtype does NOT have a significant predictive power of initial metastasis status. However, notably, the combination of the slope of change in CTC count and disease subtype has significant predictive power of initial metastasis status (AUC = 0.7922 and p-value = 0.041) (Table 10, Figures 8-11).

Furthermore, the predictive probability models of metastasis status were determined for all of the conditions:

i. The predictive probability model of metastasis status consisted of CTC change slope is as follows:

$$p = \frac{\exp\left(-0.5166 - 0.9171 \text{ X CTC change slope}\right)}{1 + \exp\left(-0.5166 - 0.9171 \text{ X CTC change slope}\right)}$$

ii. The predictive probability model of metastasis status consisting of CTCC change slope is as follows:

$$p = \frac{\exp\left(-0.3694 + 0.0344 \text{ X CTCC change slope}\right)}{1 + \exp\left(-0.3694 + 0.0344 \text{ X CTCC change slope}\right)}$$

iii. The predictive probability model of metastasis status consisted of CTC change slope and disease subtype is as follows:

$$\boldsymbol{p = \frac{\exp\left(-1.4376 - 0.9764 \text{ X CTC change slope} + 0.4198 \text{ X Disease type}\right)}{1 + \exp\left(-1.4376 - 0.9764 \text{ X CTC change slope} + 0.4198 \text{ X Disease type}\right)}}$$

iv. The predictive probability model of metastasis status consisted of CTCC change slope and disease subtype is as follows:

$$p = \frac{\exp\left(-1.3533 + 0.0264 \text{ X CTCC change slope} + 0.4327 \text{ X Disease type}\right)}{1 + \exp\left(-1.3533 + 0.0264 \text{ X CTCC change slope} + 0.4327 \text{ X Disease type}\right)}$$

In detection methodology development, there is always an aim to maximize sensitivity and specificity. Different thresholds can be used to result in different sensitivities and specificities, some of which are shown in Table 11.

Discussion

Prior to this project, there has been no published literature investigating the potential clinical utility of CTCs and CTCCs for MB patients. In this study, we were able to successfully isolate CTCs and CTCCs, which highlights the sensitivity of our nanoparticle-based detection methodology. The results of this study further show that there is a statistically significant correlation between a patient's CTC concentration and metastasis status ($r=0.24100$, $p=0.0477$) according to the Pearson Correlation test. This is consistent with previous literature findings that metastasis occurs through the movement of circulating tumor cells [5, 15]; thus, it follows that different levels of CTCs would be detected in different stages of metastasis. Higher CTC concentrations were hypothesized to correspond with more aggressive metastatic tendencies, which were indeed supported by the findings of this study.

Furthermore, ROC analysis was conducted to determine a predictive threshold for a patient's initial MB status based on CTC concentrations. It appears that the combination of the slope of change in CTC concentration and disease subtype offers significant predictive power of initial metastasis status ($AUC=0.7922$, $p=0.0410$). The inclusion of both variables in the predictive model effectively combines assessment markers for a patient's primary and metastatic tumors. The inclusion of disease subtypes, as opposed to using a single-predictor model of the slope of CTC change alone, provides greater predictive power, given how variable the four MB subtypes are in their metastatic nature. Clinically, it is crucial to consider the implications of a patient's MB subtype when considering prognosis and response to treatments as opposed to traditional one-size-fits-all methods for broader diseases.

Further analysis allowed for a deeper investigation into the balance of sensitivity and specificity. Sensitivity refers to a detection method's ability to correctly identify positive cases, while specificity refers to the test's ability to correctly identify negative cases. For example, a highly sensitive test indicates few false negative cases but comes at the expense of a higher number of positive cases. The choice of the optimal threshold value depends both on probabilistic

and clinical considerations. For example, if there is a concern that the prediction of metastasis status is inflated, a clinician may be interested in minimizing the false-positive rate so that s/he may set a fixed specificity (e.g., a specificity of 90% indicates a false-positive rate of 10%) and find the corresponding sensitivity from the ROC curve. If the clinician's interest is to maximize the identification of patients with metastatic disease, s/he may set a fixed sensitivity (for example, 90%) and identify the cutoff value providing this sensitivity in the ROC. The different threshold points of biomarkers or the additive value of multiple biomarkers to achieve specific values of sensitivity and specificity were summarized in Table 10. If the weight of sensitivity is deemed comparable to that of specificity, one can use the coordinates of the ROC curve to identify the cutoff that maximizes the sum of sensitivity and specificity.

For example, with CTC change slope alone, a cutoff point (CTC change slope Threshold ≥0.88) will achieve a sensitivity of at least 90% and a corresponding specificity of 18%. On the other hand, a cutoff point (CTC change slope ≤ -0.33) will achieve a specificity of at least 90% and a corresponding sensitivity of 57%. When an MB patient corresponds with a CTC change slope ≤ -0.773, the patient has ≥ 50% to have initial metastasis. When the cutoff threshold is 0.0026, then the sensitivity is 71% and the specificity is 82%, such that the sum of sensitivity and specificity is maximized (71%+82% = 153%). The interpretation is similar to the predictive model with CTCC change slope only.

With the combination of the slope of CTC change and disease subtype, the cutoff point (Threshold =0.9764 X CTC change slope+0.4198 X Disease type ≤ -0.438) will achieve a sensitivity of at least 90% and a specificity of 10%. On the other hand, a cutoff point (Threshold =0.9764 X CTC change slope+0.4198 X Disease type ≥ 1.19) will achieve a specificity of at least 90% and a corresponding sensitivity of 71%. When a patient with its Threshold =0.9764 X CTC change slope+0.4198 X Disease type ≥1.535, the patient has ≥ 50% to have initial metastasis. When the cutoff threshold of the combination (=0.9764 X CTC change slope+0.4198 X Disease type) is 1.26, then the sensitivity is 71% and the specificity is close to 100% so that the sum of

sensitivity and specificity is maximized (71%+100% = 171%). The interpretation is similar to the predictive model with a combination of the slope of CTCC change and disease subtype.

Interestingly, no significant correlations were made with the CTCC dataset. This outcome is likely the result of the rarity of CTCCs, which account for about 3% of the abundance of CTCs [41]. As such, it becomes difficult to assess any significant differences in the concentration of CTCCs among our samples.

One major limitation of this study was the limited sample size of patients. MB is inherently a rare cancer type, affecting approximately 350-500 patients per year in the U.S. [31]. Although, with great efforts, we were able to conduct a thorough investigation on 22 pediatric patients, the sample size in the current study should still be significantly expanded for more robust and significant correlations and results to be determined and validated. Additionally, we were unable to collect blood samples upon each patient's initial MB diagnosis, giving us no information about each patient's baseline CTC and CTCC counts. Therefore, all ratios and changes in CTC/CTCC concentrations were calculated using the earliest provided blood sample of each patient. However, the treatments and therapies undergone by each patient since his/her initial diagnosis may have significantly increased or decreased his/her CTC/CTCC concentration from the baseline, a factor that was not accounted for in this study. Through the continuation of this study and the continuous recruitment of new MB patients, we believe that we will be able to increase our sample size and provide baseline counts for patients with different initial MB conditions, i.e. primary tumor status, metastasis status, etc.

Furthermore, we hope to continue to optimize protocol conditions for the anti-NCAM antibody so that we are detecting CTCs and CTCCs with a multiplex biomarker methodology. Tumor heterogeneity is the hallmark of human cancer and is currently a major challenge to clinical management. Recent evidence strongly supports that the aggressive phenotypes of a tumor cell and its response to treatment can be defined by the activation of a set of oncogenic signaling pathways, or "resistance signature". As demonstrated by several clinical studies [39, 40],

multiplexed biomarkers, rather than one biomarker, should enhance accuracy in predicting the prognosis of cancer progression and significantly improve clinical decision-making. Thus, the usage of SYN and NCAM as detection biomarkers would increase the robustness of our results.

Conclusion

This study has demonstrated, for the first time, that significant correlations and potential clinical value exist for changes in CTC concentrations over the course of an MB patient's treatment and his/her metastasis status. Furthermore, a predictive probability model of metastasis status consisting of the slope of CTC concentration change and disease subtype was developed, and different predictive thresholds maximizing specificity and sensitivity for clinical use were provided. Together, with multiplexed biomarkers and increased sample size, we are hopeful that further significant correlations can be made that will allow for CTC/CTCC counts - tested through convenient, cheap, non-invasive liquid biopsies - to become standards of metastasis detection and prognosis predictors for MB, a debilitating disease that predominantly affects children every year.

Figures and Legends

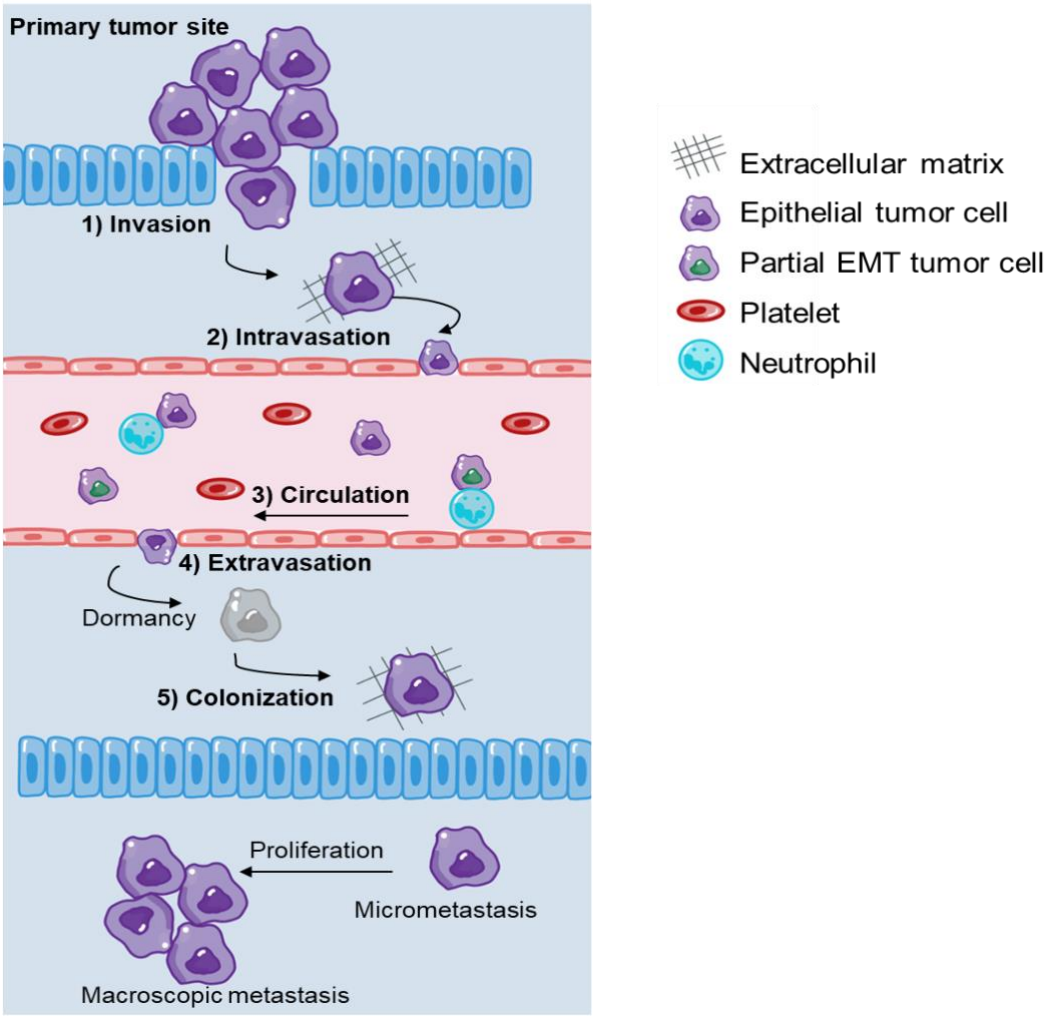

Figure 1. Mechanism of metastasis. Tumorigenic cells from the primary tumor develop mesenchymal characteristics (migratory and less adhesive) and intravasate through the wall of a blood or lymph vessel to enter circulation. Some tumorigenic cells (ex. from the epithelium) may not have fully transitioned to mesenchymal status when it enters circulation, i.e. partial epithelial-mesenchymal transition (EMT) tumor cells. Cells that are able to evade immunological defenses and mechanical stress extravasate into the extracellular matrix; some cells enter dormancy as a method of adaptation upon reaching a new microenvironment. Metastasis results.

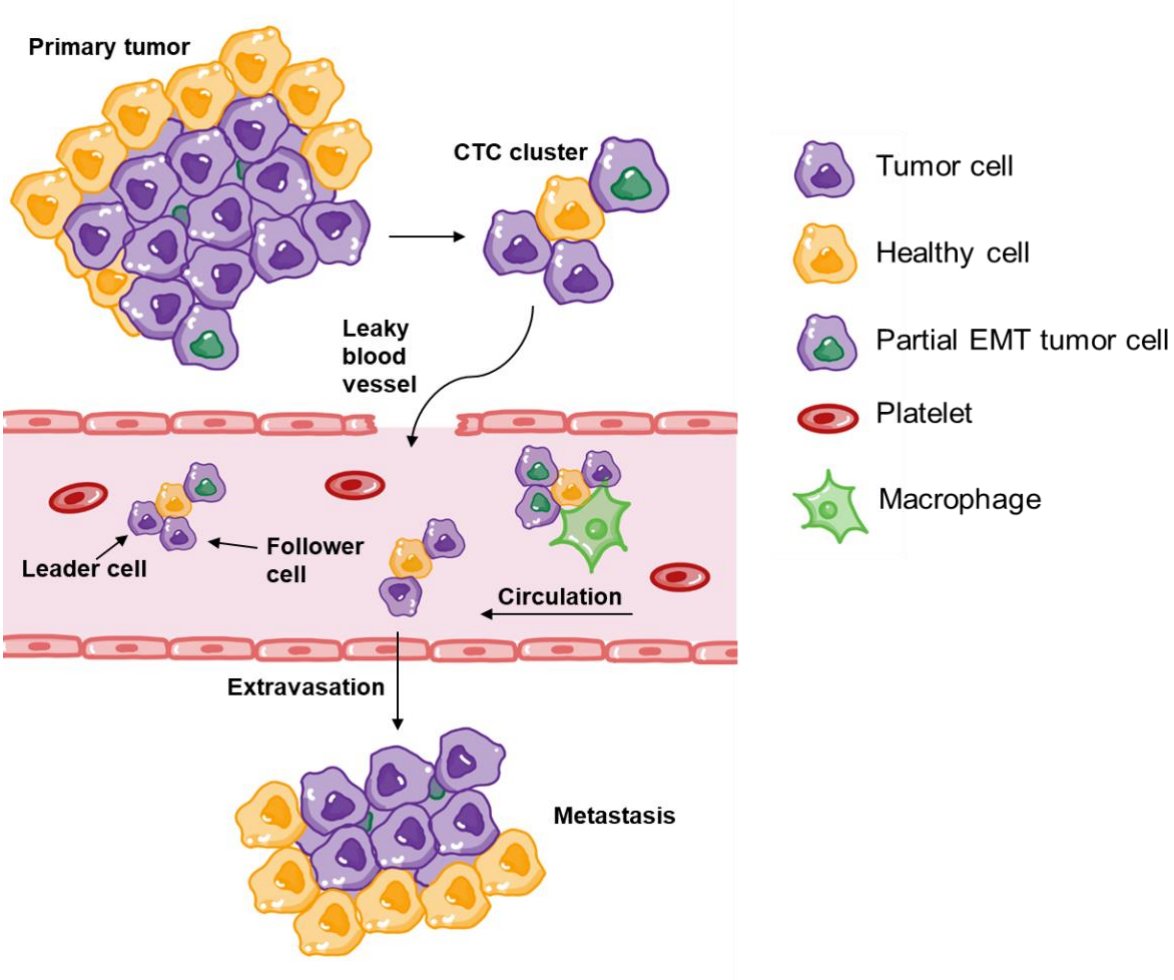

Figure 2. Mechanism of CTCC metastasis. Clusters of tumorigenic cells slough off the primary tumor and remain attached via cell-cell junctions. Leaky blood vessels allow for the intravasation of these clusters, which enter circulation. CTCCs that are able to avoid immune responses and mechanical stress travel via collective migration, in which clusters are guided by “leader” cells. Clusters circulate, extravasate, and lodge in peripheral tissue sites. Metastasis results.

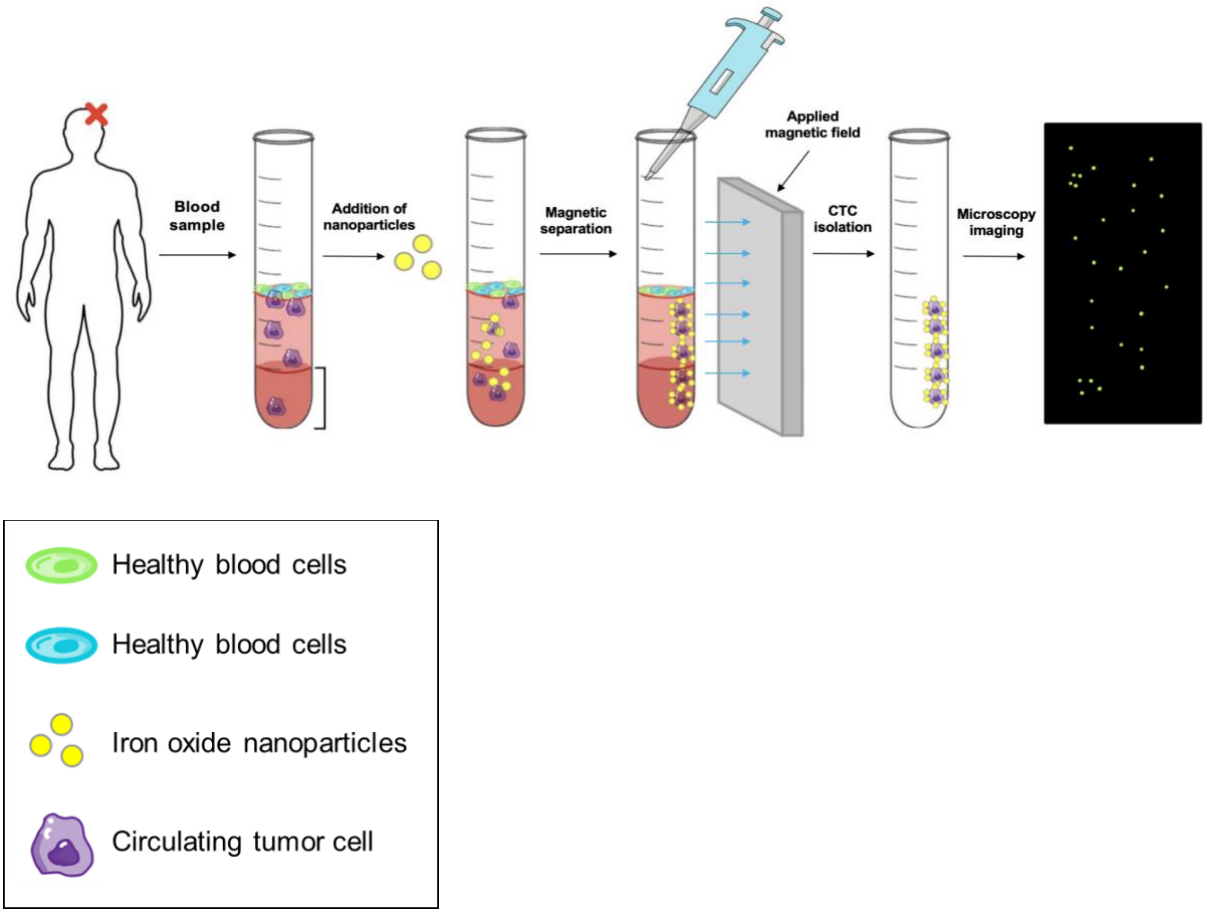

Figure 3. Design of CTC/CTCC isolation and enrichment via iron oxide technology. Blood samples are collected from medulloblastoma patients, which includes CTCs/CTCCs. Antibody-conjugated magnetic iron oxide nanoparticles are added to the blood sample, allowing nanoparticle-CTC/CTCC attachment to occur. A magnetic field is applied to the sample, separating the nanoparticle-conjugated CTCs/CTCCs from non-tumorigenic cells. The isolated cells are analyzed using microscopy and further techniques.

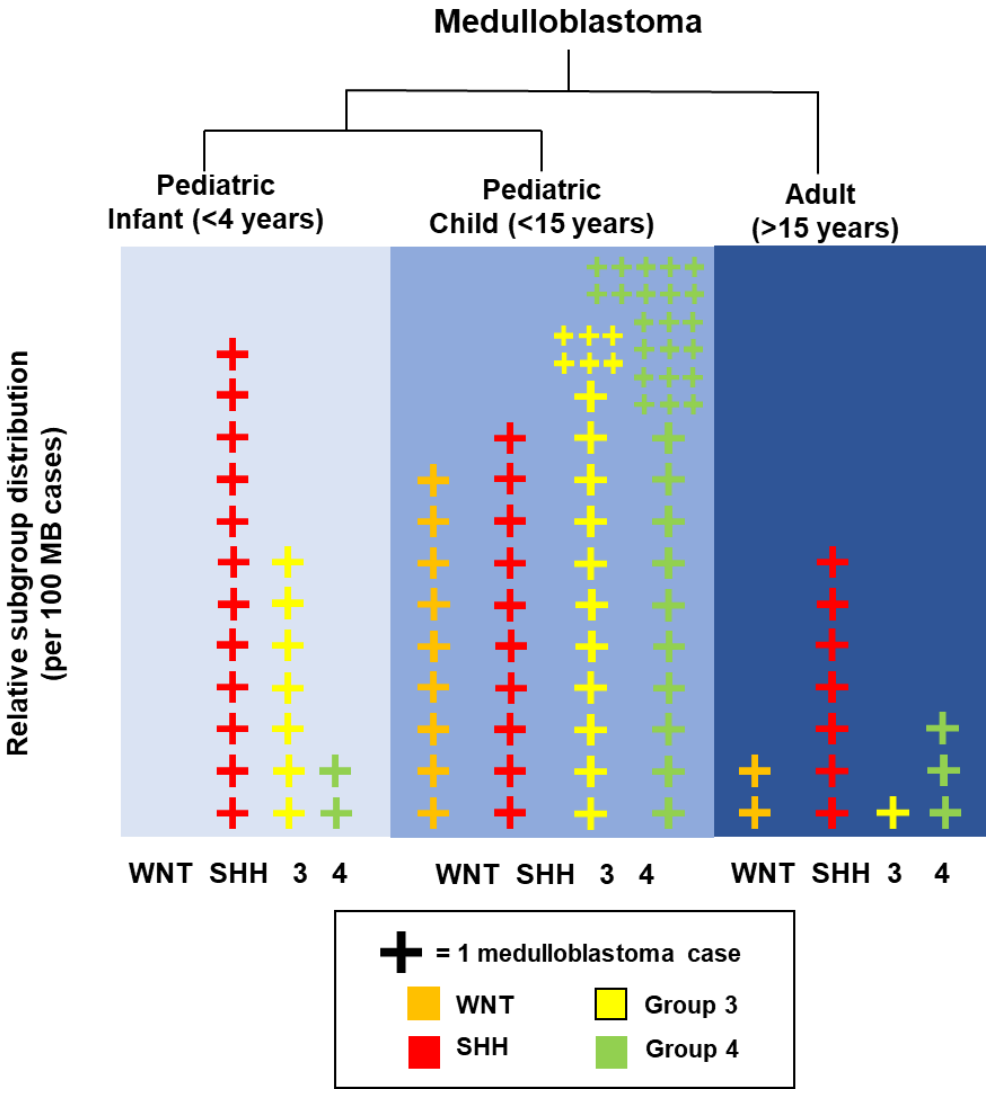

Figure 4. Relative frequencies of the 4 subtypes (WNT, Sonic Hedgehog, Group 3, Group 4) of medulloblastoma per 100 medulloblastoma tumor cases classified across 3 age categories. These 3 categories are: infants (≤4 years old), children (4-15 years old), and adults (≥15 years old), which demonstrates the differential impact and associations of each subtype on different age groups [34].

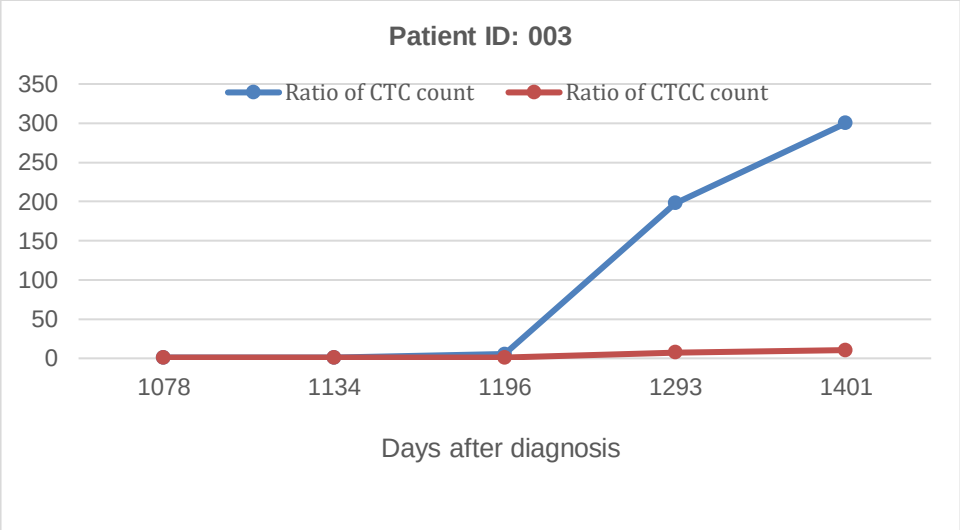
Patient ID: 003
Ratio of CTC count
Ratio of CTCC count
350
300
250
200
150
100
50
0
1078
1134
1196
1293
1401
Days after diagnosis

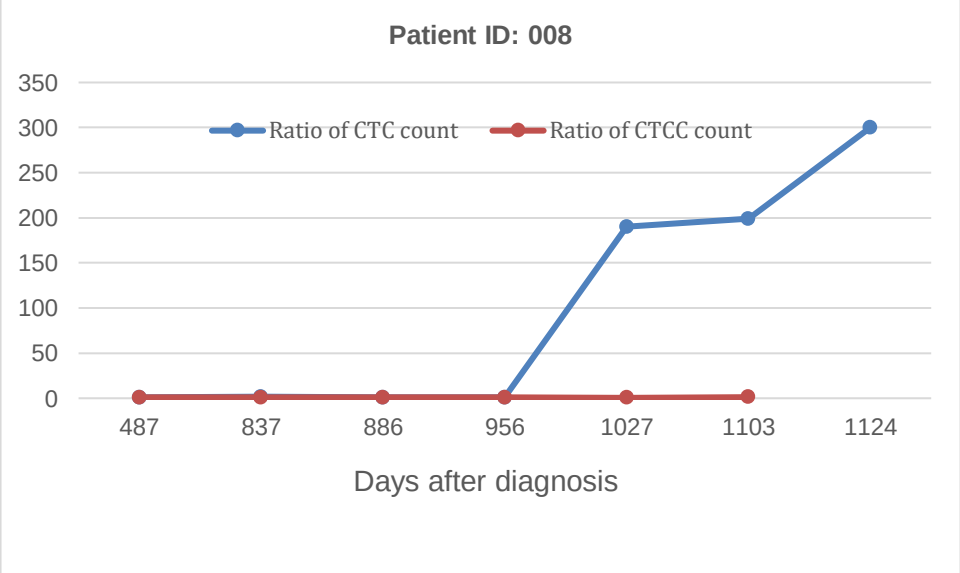
Patient ID: 008
Ratio of CTC count
Ratio of CTCC count
350
300
250
200
150
100
50
0
487
837
886
956
1027
1103
1124
Days after diagnosis

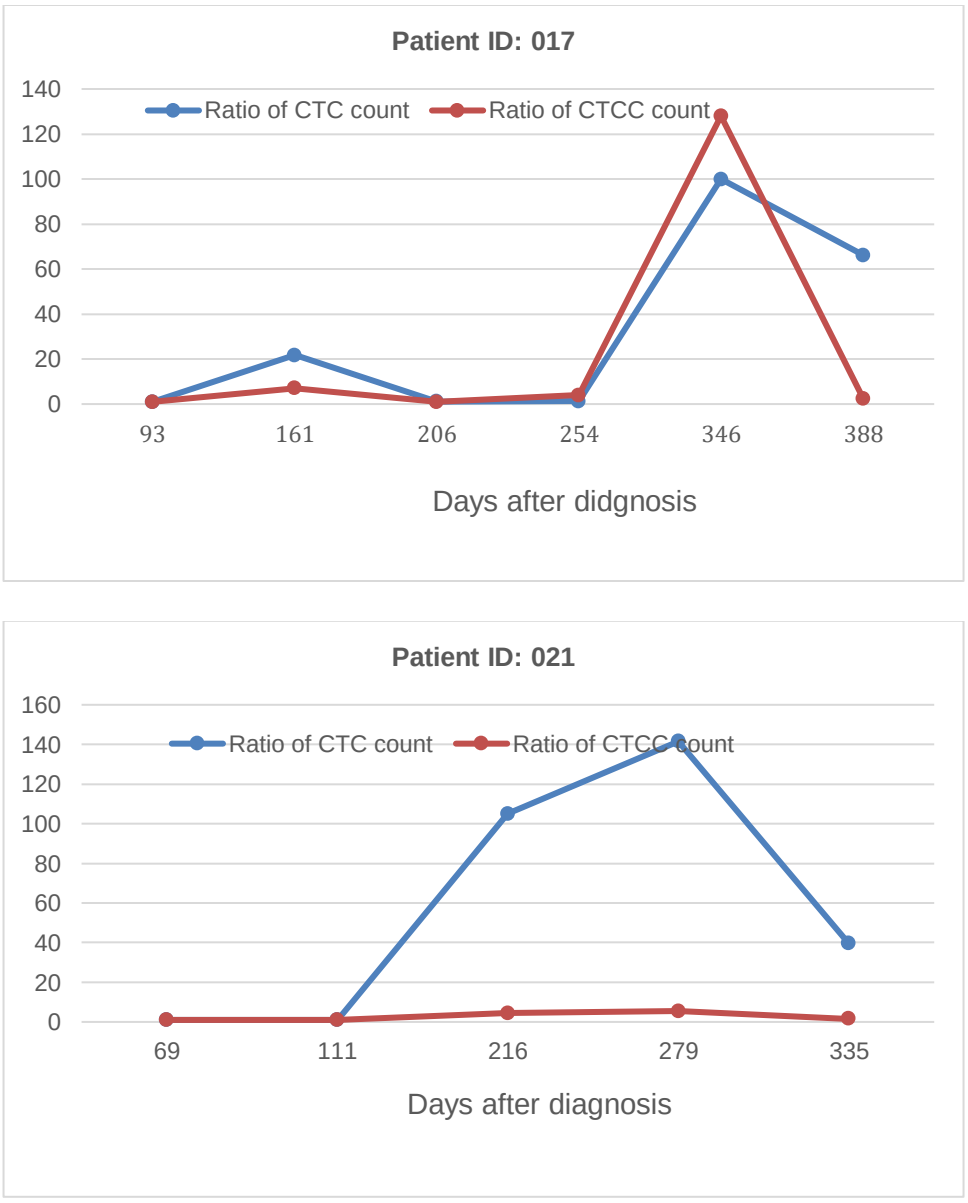

Figure 5. Schedule for CTC/CTCC detection and the relative ratio of change in CTC/CTCC counts in four MB patients enrolled in the current study.

a)

b)

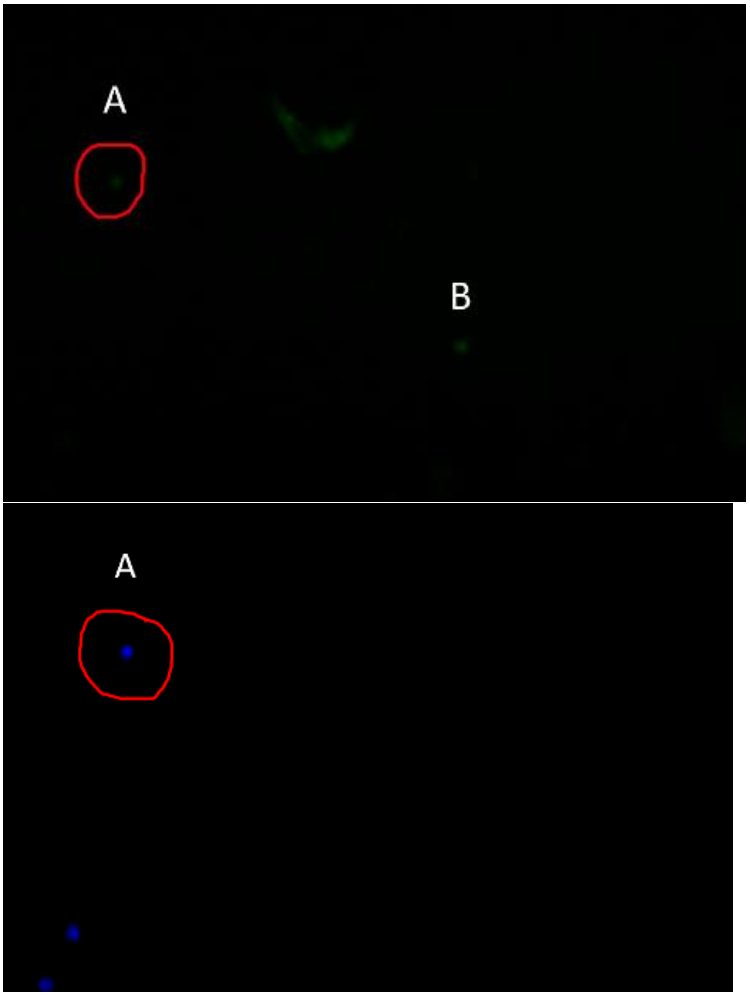

Figure 6. a) CTC microscopy image of FITC-labeled anti-synaptophysin (anti-SYN) with Alexa Fluor 488 antibody. Two positive signals for SYN are shown: A and B. Only A is identified as a CTC due to a corresponding positive signal in the DAPI-stained channel image **b)** CTC microscopy image of DAPI-stained cells.

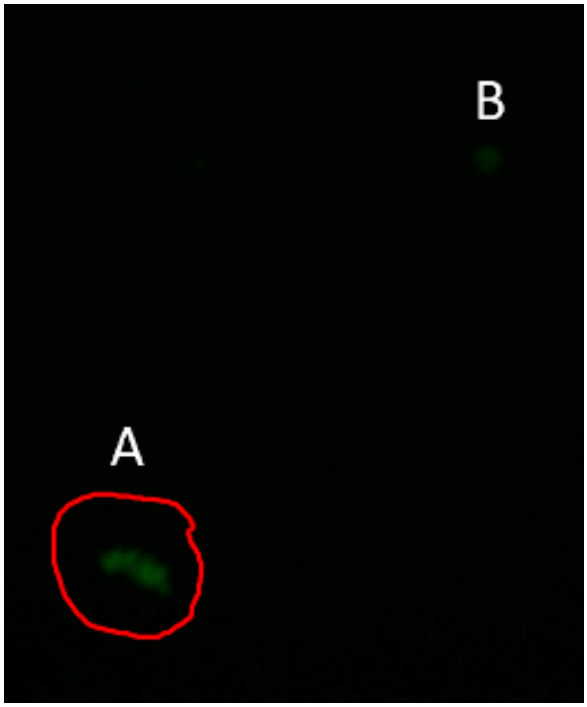

Figure 7. CTCC microscopy image of FITC-labeled anti-synaptophysin (anti-SYN) with Alexa Fluor 488 antibody.

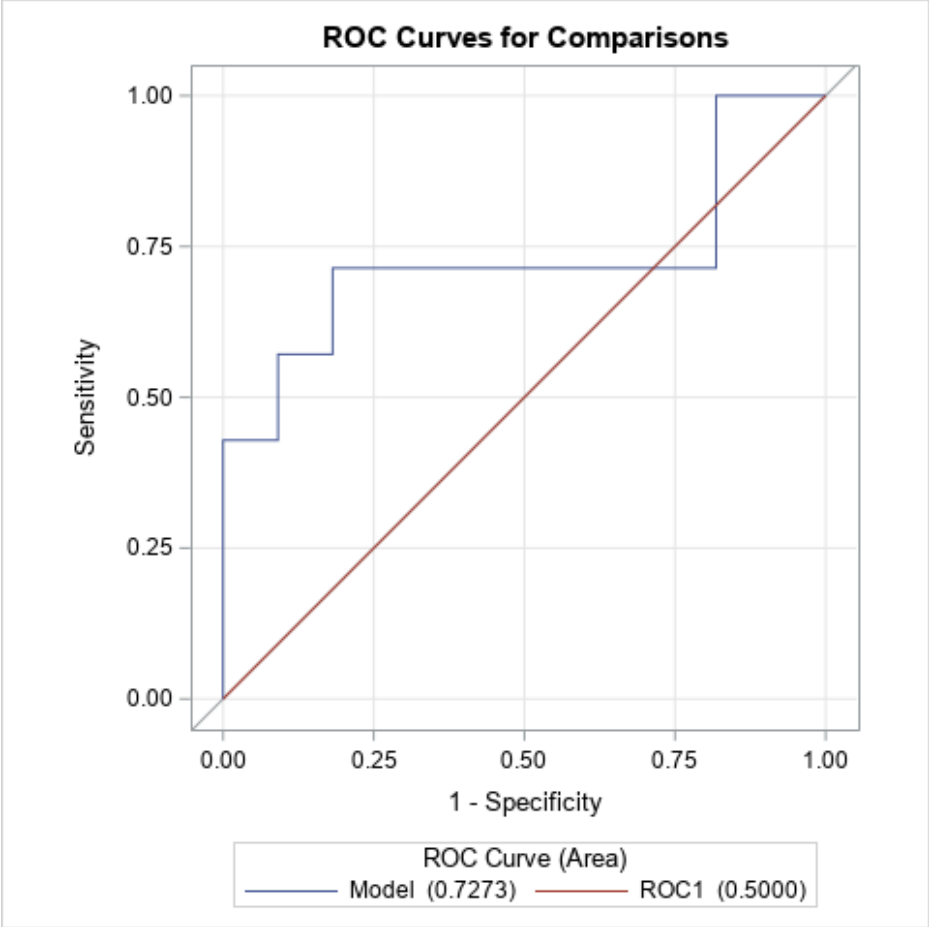

Figure 8. ROC curves for the slope of change in CTC counts over the course of a patient's treatment as a predictor of the patient's initial metastasis status.

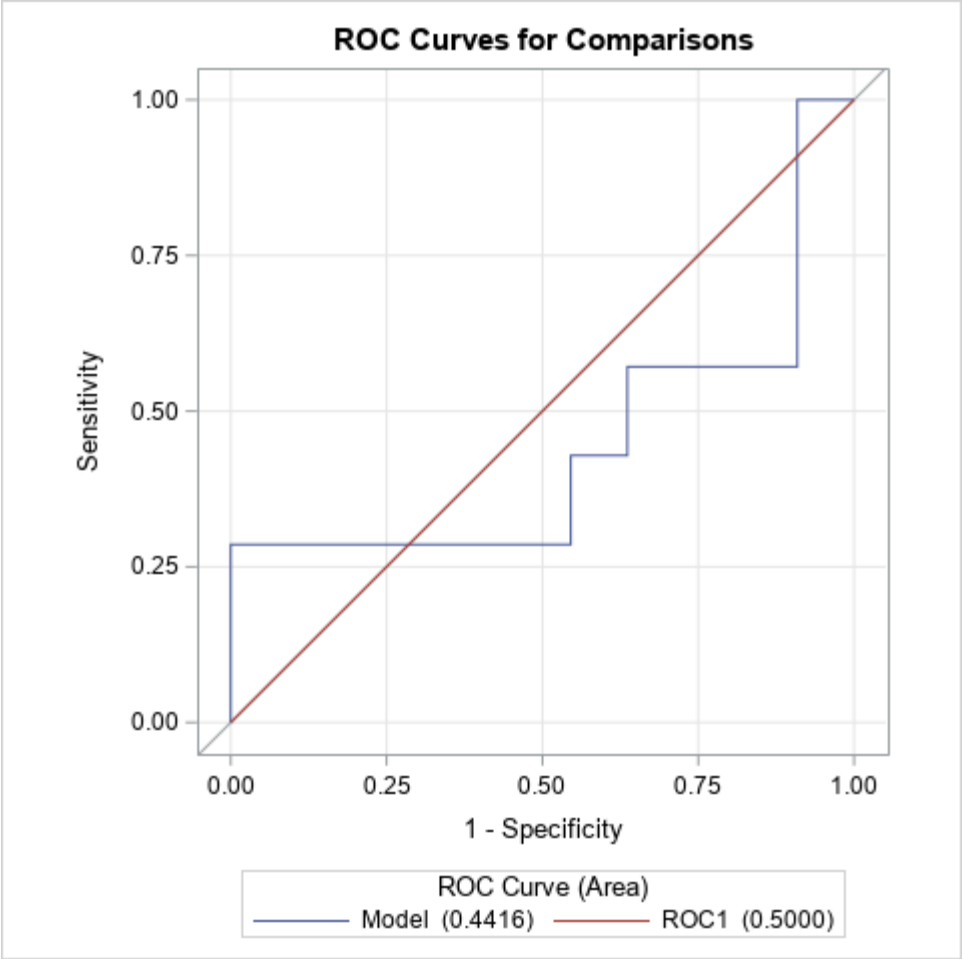

Figure 9. ROC curves for the slope of change in CTCC counts over the course of a patient's treatment as a patient's initial metastasis status.

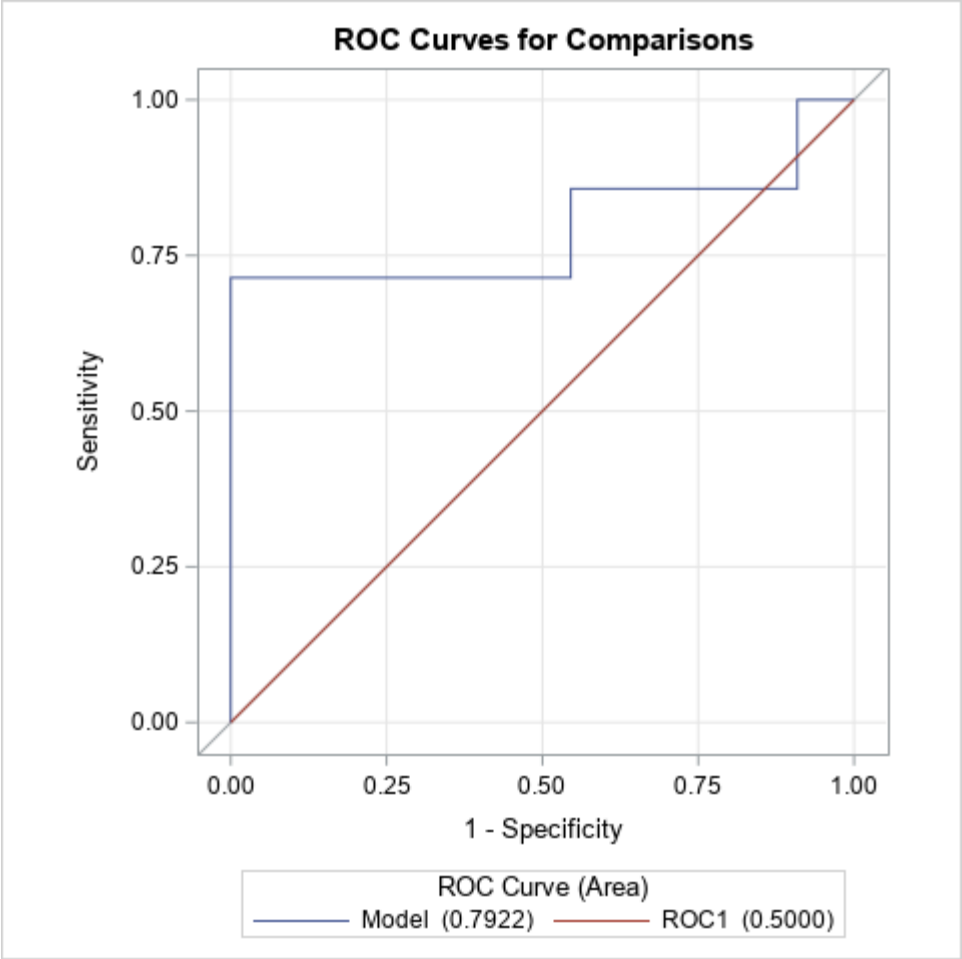

Figure 10. ROC curves for the combination of disease subtype (WNT, SHH, Group 3/4) and slope of change in CTC counts over the course of a patient's treatment as predictors of the patient's initial metastasis status.

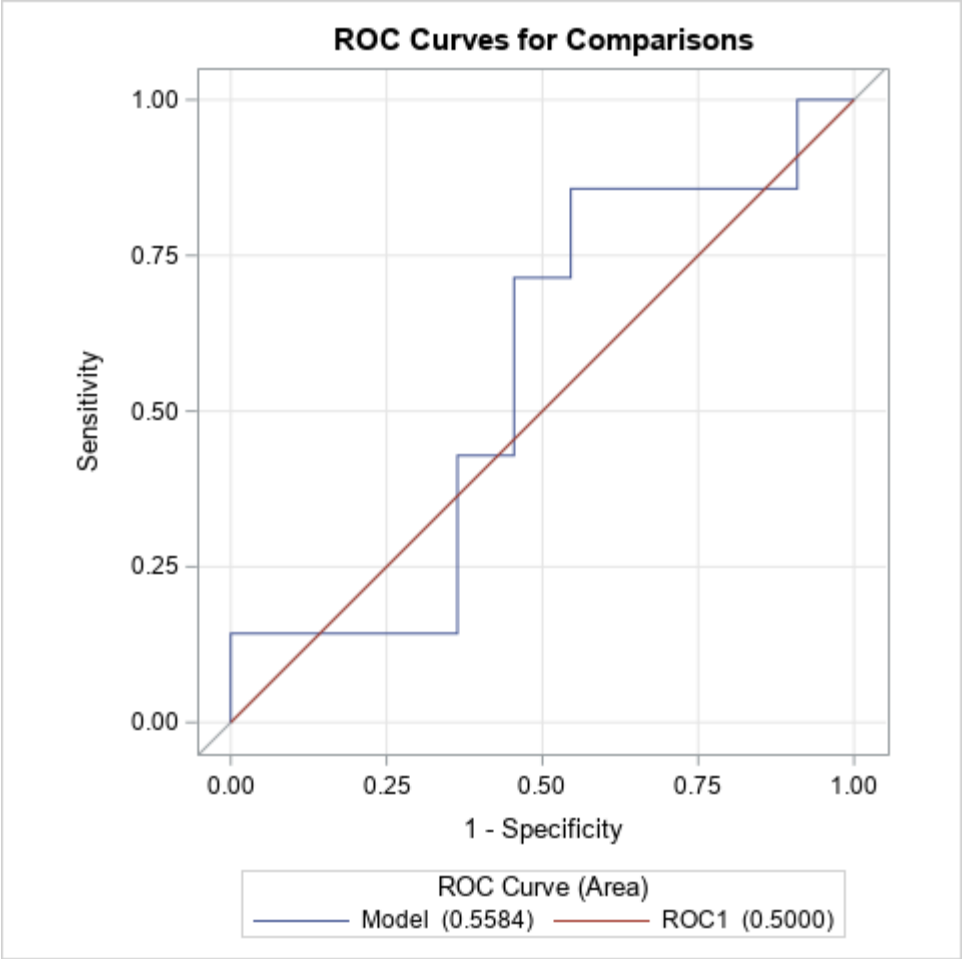

Figure 11. ROC curves for combination of disease subtype (WNT, SHH, Group 3/4) and slope of change in CTCC counts over the course of a patient's treatment as predictors of the patient's initial metastasis status.

Table 1. Comparison of the four subtypes of medulloblastoma based on demographic characteristics (age groups and gender), clinical features (histology, metastasis, prognosis), and genetics (gene alterations and expression) [34].

Medulloblastoma Molecular and Clinical Subtypes							
	Demographics		**Clinical Features**			**Genetics**	
MB Subtype	**Age Group**	**Gender**	**Histology**	**Metastasis (M0 or M+)**	**Prognosis**	**Alterations**	**Gene Expression**
WNT	Child, adult	♂♂:♀♀	Classic, rarely LCA	Rarely M+	Very good	*CTNBB1* mutation	WNT signaling; MYC+
SHH	All; mostly infants	♂♂:♀♀	Desmoplastic/ nodular, classic, LCA	Uncommon M+	Infants good; others intermediate	*PTCH1/SMO/ SUFU* mutation*; GL12* amplification; *MYCN* amplification	SHH signaling; MYCN+
Group 3	Infant, child; mostly children	♂♂:♀	Classic, LCA	Very frequently M+	Poor	*MYC* amplification	Photoreceptor/ GABAergic; MYC+++
Group 4	All; mostly children	♂♂:♀	Classic, LCA	Frequently M+	Intermediate	*CDK6* amplification; *MYCN* amplification	Neuronal/ glutamatergic; minimal MYC/MYCN

Table 2. Patient cohort characterization.

Variable	**All Cases (N=32)**
Age (yrs)	
1-5	7 (21.9%)
6-10	14 (43.8%)
11-15	6 (18.8%)
16-17	2 (6.3%)
≥18	3 (9.4%)
Disease Subtype	
N/A (negative control)	10 (31.3%)
SHH	8 (25%)
WNT	1 (3.1%)
Group 3/4	13 (40.6%)
M Stage at Diagnosis	
N/A (negative control)	10 (31.3%)
M0	14 (43.8%)
M1	2 (6.3%)
M2	1 (3.1%)
M3	5 (15.6%)

Table 3. Descriptive statistics of CTC and CTCC Enumeration based on FITC-labeled and DAPI images

Variables	**N**	**Mean**	**SD**	**Median**	**Range**
CTC Count	69	90.85	112.71	1	0 – 300+
CTC Ratio	69	39.53	82.18	1	0 – 300+
Slope of CTC Change	18	-0.7057	3.6887	0.07235	-15.25 – 1.2102
CTCC Count	67	9.22	24.63	2	0 – 150
CTCC Ratio	67	4.63	16.04	1	0 – 128
Slope of CTCC Change	18	-3.1265	11.48	0.0036	-48.35 – 1

Table 4. Frequencies of primary tumor statuses according to the CTC dataset. NED/CCR = no evidence of disease/continued complete remission; R1 = first relapse; R2 = second relapse; R3 = third relapse; No change = primary tumor present but no change in status.

Primary Status				
Primary Tumor Status	**Frequency**	**Percent (%)**	**Cumulative Frequency**	**Cumulative Percent (%)**
NED/CCR	14	20.29	14	20.29
R1	20	28.99	34	49.28
R2	4	5.80	38	55.07
R3	3	4.35	41	59.42
No change	28	40.58	69	100.00

Table 5. Frequencies of metastasis status according to the CTC dataset. M0 = no evidence of metastasis; M1-3 = presence of metastasis of increasing aggressiveness.

Metastasis				
Metastasis Status	**Frequency**	**Percentage (%)**	**Cumulative Frequency**	**Cumulative Percentage (%)**
0	36	52.94	36	52.94
1	4	5.88	40	58.82
2	5	7.35	45	66.18
3	23	33.82	68	100.00
Frequency Missing = 1				

Table 6. Frequencies of metastasis status upon medulloblastoma diagnosis according to the CTC dataset.

Initial M status				
Initial M Status	**Frequency**	**Percentage (%)**	**Cumulative Frequency**	**Cumulative Percentage (%)**
0	43	62.32	43	62.32
1	5	7.25	48	69.57
2	3	4.35	51	73.91
3	18	26.09	69	100.00

Table 7. Frequencies of the 4 medulloblastoma subtypes according to the CTC dataset: SHH (Sonic Hedgehog), WNT, and Groups 3 and 4.

Disease Subtype (SHH=1, WNT=2, Group 3/4=3)				
Disease Subtype	**Frequency**	**Percentage (%)**	**Cumulative Frequency**	**Cumulative Percentage (%)**
SHH = 1	26	37.68	26	37.68
WNT = 2	3	4.35	29	42.03
Group 3/4=3	40	57.97	69	100.00

Table 8. Correlations of CTC count (CTC/mL blood) and CTC ratio with primary tumor status or metastasis status.

	Primary Tumor Status		Metastasis status	
	Pearson Correlation Coefficient	**Spearman Correlation Coefficient**	**Pearson Correlation Coefficient**	**Spearman Correlation Coefficient**
CTC count	r = 0.07069 p = 0.5638	r = -0.01615 p = 0.8952	**r = 0.24100** **p = 0.0477**	r = 0.13915 p = 0.2577
CTC ratio	r = 0.02009 p = 0.8699	r = -0.15369 p = 0.2074	r = 0.17234 p = 0.1599	r = 0.02166 p = 0.8608

Table 9. Correlations of CTCC count (CTCC/mL blood) and CTCC ratio with primary tumor status or metastasis status.

	Primary Tumor Status		**Metastasis status**	
	Pearson Correlation Coefficient	**Spearman Correlation Coefficient**	**Pearson Correlation Coefficient**	**Spearman Correlation Coefficient**
CTCC count	r = 0.03238 p = 0.7948	r = 0.06100 p = 0.6239	r = 0.18279 p = 0.1418	r = -0.04283 p = 0.7327
CTCC ratio	r = -0.06005 p = 0.6293	r = -0.05090 p = 0.6825	r = 0.10264 p = 0.4122	r = -0.18224 p = 0.1430

Table 10. ROC analysis of biomarkers using single-predictor modeling (slope of change in CTC count OR slope of change in CTCC count) and two-predictor modeling (slope of change in CTC count + disease type OR slope of change in CTCC count + disease type)

Parameter	Area under ROC curve	Standard Error	(95%Wald Confidence Interval)		p-value
			Lower Limit	Upper Limit	
Single Predictor Model					
CTC Change Slope	0.7273	0.1512	0.4309	1.0000	0.1328
CTCC Change Slope	0.4416	0.1685	0.1112	0.7719	0.7288
Two Predictor Model					
CTC Change Slope + Disease type	**0.7922**	0.1430	0.5120	1.0000	**0.0410**
CTCC Change Slope + Disease type	0.5584	0.1486	0.2673	0.8496	0.6940

Table 11. A summary of the threshold for different sensitivities and specificities based on different models.

Parameter	Sensitivity > 90%	Specificity> 90%	Maximize sum of specificity and sensitivity	≥ 50% to be Initial Metastasis
CTC change slope	**Specificity=18% Threshold=0.88**	**Sensitivity=57% Threshold = -0.33**	**Sensitivity=71% Specificity=82% Threshold =0.0026**	**CTC threshold < = -0.773**
CTCC change slope	Sensitivity = 83% Specificity=50% Threshold = 1.27	Specificity=93% Sensitivity = 61% Threshold = 0.93	Sensitivity=61% Specificity=100% Threshold = 0.84	CTCC Threshold <=1.15
Threshold =0.9764 X CTC change slope + 0.4198 X Disease type				
Threshold =0.0264 X CTCC change slope + 0.4327 X Disease type	Sensitivity = 89% Specificity=79% Threshold =-1.50	Specificity=93% Sensitivity=55% Threshold =0.78	Sensitivity=100% Specificity=86% Threshold = -1.64	Threshold ≥- 1.54

References Cited

[1] R.L. Siegel, K.D. Miller, N.S. Wagle, A. Jemal, Cancer statistics, 2023, CA Cancer J Clin, 73 (2023) 17-48.
[2] A.C. Chiang, J. Massague, Molecular basis of metastasis, N Engl J Med, 359 (2008) 2814-2823.
[3] J. Majidpoor, K. Mortezaee, Steps in metastasis: an updated review, Med Oncol, 38 (2021) 3.
[4] P. Carmeliet, R.K. Jain, Principles and mechanisms of vessel normalization for cancer and other angiogenic diseases, Nat Rev Drug Discov, 10 (2011) 417-427.
[5] H. Dianat-Moghadam, M. Azizi, S.Z. Eslami, L.E. Cortes-Hernandez, M. Heidarifard, M. Nouri, C. Alix-Panabieres, The Role of Circulating Tumor Cells in the Metastatic Cascade: Biology, Technical Challenges, and Clinical Relevance, Cancers (Basel), 12 (2020).
[6] K. Pantel, M.R. Speicher, The biology of circulating tumor cells, Oncogene, 35 (2016) 1216-1224.
[7] J. Fares, M.Y. Fares, H.H. Khachfe, H.A. Salhab, Y. Fares, Molecular principles of metastasis: a hallmark of cancer revisited, Signal Transduct Target Ther, 5 (2020) 28.
[8] T. Mazard, L. Cayrefourcq, F. Perriard, H. Senellart, B. Linot, C. de la Fouchardiere, E. Terrebonne, E. Francois, S. Obled, R. Guimbaud, L. Mineur, M. Fonck, J.P. Daures, M. Ychou, E. Assenat, C. Alix-Panabieres, Clinical Relevance of Viable Circulating Tumor Cells in Patients with Metastatic Colorectal Cancer: The COLOSPOT Prospective Study, Cancers (Basel), 13 (2021).
[9] S. Amintas, A. Bedel, F. Moreau-Gaudry, J. Boutin, L. Buscail, J.P. Merlio, V. Vendrely, S. Dabernat, E. Buscail, Circulating Tumor Cell Clusters: United We Stand Divided We Fall, Int J Mol Sci, 21 (2020).
[10] H. Thangavel, C. De Angelis, S. Vasaikar, R. Bhat, M.K. Jolly, C. Nagi, C.J. Creighton, F. Chen, L.E. Dobrolecki, J.T. George, T. Kumar, N.M. Abdulkareem, S. Mao, A. Nardone, M. Rimawi, C.K. Osborne, M.T. Lewis, H. Levine, B. Zhang, R. Schiff, M. Giuliano, M.V. Trivedi, A CTC-Cluster-Specific Signature Derived from OMICS Analysis of Patient-Derived Xenograft Tumors Predicts Outcomes in Basal-Like Breast Cancer, J Clin Med, 8 (2019).
[11] Y. Yang, H. Zheng, Y. Zhan, S. Fan, An emerging tumor invasion mechanism about the collective cell migration, Am J Transl Res, 11 (2019) 5301-5312.
[12] K.J. Cheung, V. Padmanaban, V. Silvestri, K. Schipper, J.D. Cohen, A.N. Fairchild, M.A. Gorin, J.E. Verdone, K.J. Pienta, J.S. Bader, A.J. Ewald, Polyclonal breast cancer metastases arise from collective dissemination of keratin 14-expressing tumor cell clusters, Proc Natl Acad Sci U S A, 113 (2016) E854-863.
[13] R.H. Eibl, M. Schneemann, Liquid Biopsy and Primary Brain Tumors, Cancers (Basel), 13 (2021).
[14] A. Snow, D. Chen, J.E. Lang, The current status of the clinical utility of liquid biopsies in cancer, Expert Rev Mol Diagn, 19 (2019) 1031-1041.
[15] D. Lin, L. Shen, M. Luo, K. Zhang, J. Li, Q. Yang, F. Zhu, D. Zhou, S. Zheng, Y. Chen, J. Zhou, Circulating tumor cells: biology and clinical significance, Signal Transduct Target Ther, 6 (2021) 404.
[16] S. Nagrath, L.V. Sequist, S. Maheswaran, D.W. Bell, D. Irimia, L. Ulkus, M.R. Smith, E.L. Kwak, S. Digumarthy, A. Muzikansky, P. Ryan, U.J. Balis, R.G. Tompkins, D.A. Haber, M. Toner, Isolation of rare circulating tumour cells in cancer patients by microchip technology, Nature, 450 (2007) 1235-1239.
[17] F.Z. Shahneh, Sensitive antibody-based CTCs detection from peripheral blood, Hum Antibodies, 22 (2013) 51-54.
[18] H. Wang, J. Wu, Q. Zhang, J. Hao, Y. Wang, Z. Li, H. Niu, H. Zhang, S. Zhang, A Modified Method to Isolate Circulating Tumor Cells and Identify by a Panel of Gene Mutations in Lung Cancer, Technol Cancer Res Treat, 20 (2021) 1533033821995275.
[19] Z. Liu, A. Fusi, E. Klopocki, A. Schmittel, I. Tinhofer, A. Nonnenmacher, U. Keilholz, Negative enrichment by immunomagnetic nanobeads for unbiased characterization of circulating tumor cells from peripheral blood of cancer patients, J Transl Med, 9 (2011) 70.

[20] R.H. Eibl, M. Schneemann, Medulloblastoma: From TP53 Mutations to Molecular Classification and Liquid Biopsy, Biology (Basel), 12 (2023).
[21] Q. Zhang, K. Hou, H. Chen, N. Zeng, Y. Wu, Nanotech Probes: A Revolution in Cancer Diagnosis, Front Oncol, 12 (2022) 933125.
[22] Y. Liu, R. Li, L. Zhang, S. Guo, Nanomaterial-Based Immunocapture Platforms for the Recognition, Isolation, and Detection of Circulating Tumor Cells, Front Bioeng Biotechnol, 10 (2022) 850241.
[23] P. Liu, P. Jonkheijm, L. Terstappen, M. Stevens, Magnetic Particles for CTC Enrichment, Cancers (Basel), 12 (2020).
[24] S.C. Tsao, J. Wang, Y. Wang, A. Behren, J. Cebon, M. Trau, Characterising the phenotypic evolution of circulating tumour cells during treatment, Nat Commun, 9 (2018) 1482.
[25] H. Lee, M. Choi, J. Lim, M. Jo, J.Y. Han, T.M. Kim, Y. Cho, Magnetic Nanowire Networks for Dual-Isolation and Detection of Tumor-Associated Circulating Biomarkers, Theranostics, 8 (2018) 505-517.
[26] C.W. Kuo, D.Y. Chueh, P. Chen, Real-time in vivo imaging of subpopulations of circulating tumor cells using antibody conjugated quantum dots, J Nanobiotechnology, 17 (2019) 26.
[27] P. Farinha, J.M.P. Coelho, C.P. Reis, M.M. Gaspar, A Comprehensive Updated Review on Magnetic Nanoparticles in Diagnostics, Nanomaterials (Basel), 11 (2021).
[28] P.R.S. Baabu, H.K. Kumar, M.B. Gumpu, K.J. Babu, A.J. Kulandaisamy, J.B.B. Rayappan, Iron Oxide Nanoparticles: A Review on the Province of Its Compounds, Properties and Biological Applications, Materials (Basel), 16 (2022).
[29] J.Y. Choi, Medulloblastoma: Current Perspectives and Recent Advances, Brain Tumor Res Treat, 11 (2023) 28-38.
[30] M.J. Hossain, W. Xiao, M. Tayeb, S. Khan, Epidemiology and prognostic factors of pediatric brain tumor survival in the US: Evidence from four decades of population data, Cancer Epidemiol, 72 (2021) 101942.
[31] N.E. Millard, K.C. De Braganca, Medulloblastoma, J Child Neurol, 31 (2016) 1341-1353.
[32] L. Garzia, N. Kijima, A.S. Morrissy, P. De Antonellis, A. Guerreiro-Stucklin, B.L. Holgado, X. Wu, X. Wang, M. Parsons, K. Zayne, A. Manno, C. Kuzan-Fischer, C. Nor, L.K. Donovan, J. Liu, L. Qin, A. Garancher, K.W. Liu, S. Mansouri, B. Luu, Y.Y. Thompson, V. Ramaswamy, J. Peacock, H. Farooq, P. Skowron, D.J.H. Shih, A. Li, S. Ensan, C.S. Robbins, M. Cybulsky, S. Mitra, Y. Ma, R. Moore, A. Mungall, Y.J. Cho, W.A. Weiss, J.A. Chan, C.E. Hawkins, M. Massimino, N. Jabado, M. Zapotocky, D. Sumerauer, E. Bouffet, P. Dirks, U. Tabori, P.H.B. Sorensen, P.K. Brastianos, K. Aldape, S.J.M. Jones, M.A. Marra, J.R. Woodgett, R.J. Wechsler-Reya, D.W. Fults, M.D. Taylor, A Hematogenous Route for Medulloblastoma Leptomeningeal Metastases, Cell, 173 (2018) 1549.
[33] S. Tran, F. Bielle, WHO 2021 and beyond: new types, molecular markers and tools for brain tumor classification, Curr Opin Oncol, 34 (2022) 670-675.
[34] M.D. Taylor, P.A. Northcott, A. Korshunov, M. Remke, Y.J. Cho, S.C. Clifford, C.G. Eberhart, D.W. Parsons, S. Rutkowski, A. Gajjar, D.W. Ellison, P. Lichter, R.J. Gilbertson, S.L. Pomeroy, M. Kool, S.M. Pfister, Molecular subgroups of medulloblastoma: the current consensus, Acta Neuropathol, 123 (2012) 465-472.
[35] Medulloblastoma Circulating Tumor Cells Form Leptomeningeal Metastases, Cancer Discov, 8 (2018) 383.
[36] K. Schwechheimer, B. Wiedenmann, W.W. Franke, Synaptophysin: a reliable marker for medulloblastomas, Virchows Arch A Pathol Anat Histopathol, 411 (1987) 53-59.
[37] H.S. Min, Y.J. Lee, K. Park, B.K. Cho, S.H. Park, Medulloblastoma: histopathologic and molecular markers of anaplasia and biologic behavior, Acta Neuropathol, 112 (2006) 13-20.

[38] L. Todaro, S. Christiansen, M. Varela, P. Campodonico, M.G. Pallotta, J. Lastiri, E. Sacerdote de Lustig, E. Bal de Kier Joffe, L. Puricelli, Alteration of serum and tumoral neural cell adhesion molecule (NCAM) isoforms in patients with brain tumors, J Neurooncol, 83 (2007) 135-144.
[39] T. Landemaine, A. Jackson, A. Bellahcene, N. Rucci, S. Sin, B.M. Abad, A. Sierra, A. Boudinet, J.M. Guinebretiere, E. Ricevuto, C. Nogues, M. Briffod, I. Bieche, P. Cherel, T. Garcia, V. Castronovo, A. Teti, R. Lidereau, K. Driouch, A six-gene signature predicting breast cancer lung metastasis, Cancer Res, 68 (2008) 6092-6099.
[40] S. Vicent, D. Luis-Ravelo, I. Anton, I. Garcia-Tunon, F. Borras-Cuesta, J. Dotor, J. De Las Rivas, F. Lecanda, A novel lung cancer signature mediates metastatic bone colonization by a dual mechanism, Cancer Res, 68 (2008) 2275-2285.
[41] Q. Chen, J. Zou, Y. He, Y. Pan, G. Yang, H. Zhao, Y. Huang, Y. Zhao, A. Wang, W. Chen, Y. Lu, A narrative review of circulating tumor cells clusters: A key morphology of cancer cells in circulation promote hematogenous metastasis, Front Oncol, 12 (2022) 944487.